Magnetic Resonance in Medicine 43:368–374 (2000)

Test Liquids for Quantitative MRI Measurements of Self-Diffusion Coefficient In Vivo

P.S. Tofts,[1]* D. Lloyd,[2] C.A. Clark,[1] G.J. Barker,[1] G.J.M. Parker,[1] P. McConville,[2] C. Baldock,[2] and J.M. Pope[2]

A range of liquids suitable as quality control test objects for measuring the accuracy of clinical MRI diffusion sequences (both apparent diffusion coefficient and tensor) has been identified and characterized. The self-diffusion coefficients for 15 liquids (3 cyclic alkanes: cyclohexane to cyclooctane, 9 n-alkanes: n-octane to n-hexadecane, and 3 n-alcohols: ethanol to 1-propanol) were measured at 15–30°C using an NMR spectrometer. Values at 22°C range from 0.36 to 2.2 10^{-9} m^2s^{-1}. Typical 95% confidence limits are ±2%. Temperature coefficients are 1.7–3.2 %/°C. T_1 and T_2 values at 1.5 T and proton density are given. n-tridecane has a diffusion coefficient close to that of normal white matter. The longer n-alkanes may be useful T_2 standards. Measurements from a spin-echo MRI sequence agreed to within 2%. Magn Reson Med 43:368–374, 2000. © 2000 Wiley-Liss, Inc.

Key words: diffusion coefficient; MRI; alkane; quality control

MR diffusion imaging (1–5) is now an established technique for the investigation of brain tissue structure. It has been used to investigate brain lesions in ischemia (6), multiple sclerosis (MS) (7), epilepsy (8), and tumors (9), and has been used to study brain development (10) and fiber tract connectivity (11). Diffusion is anisotropic in white matter (12), and the apparent diffusion tensor is a mathematical description of tissue water diffusion (13) providing rotationally invariant measures of diffusion and anisotropy (14,15).

A number of instrumental factors can give rise to random or systematic errors in estimates of diffusion coefficient. Random errors arise from image noise (enhanced by signal loss due to T_2 effects, or inadequate diffusion sensitivity from low *b*-factors) and motion artifacts (arising from flow and convection effects, or motion of the sample or subject). Systematic errors can arise from incorrect values used for the diffusion gradient amplitudes, the presence of imaging, susceptibility, or eddy current gradient cross-terms unaccounted for in the *b*-value calculation, errors in the *b*-value calculation (which can be extremely complex), image noise (this can give apparent anisotropy in isotropic media) (15,16) gradient calibration inaccuracy, and lack of temperature control (in test objects).

An ideal set of materials should have the following characteristics:

i) Diffusion coefficients should cover the range found in vivo. Normal white matter has a mean apparent diffusion coefficient (ADC) of approximately 0.70–0.75 10^{-9} m^2 s^{-1} (16,17); when the tensor is measured, values range from 0.3–1.0 10^{-9} m^2 s^{-1} (17). Ischemic brain has ADC values down to 0.4 10^{-9} m^2 s^{-1} (16). In MS, values can increase to 2.1 10^{-9} m^2 s^{-1} (18). Thus, a range of 0.3–2.1 10^{-9} m^2 s^{-1} at room temperature would be appropriate for a set of test objects.

ii) The set of materials should be easily obtainable world-wide, with minimal on-site preparation required. The set should be stable, cheap, and nontoxic.

iii) Each material should have a single proton NMR spectral line (as does the brain, predominantly). Multiple lines (such as fat in the cranium) can cause two problems. Firstly, all but one of the lines must be suppressed for echo-planar imaging and, secondly, J-modulation leads to partial signal cancellation in a spin-echo train.

iv) Each material should have values of T_1 and T_2 that are comparable with in vivo values (i.e., $T_1 \approx 720$ms, $T_2 \approx$ 90 msec at 1.5 T in white matter; 19). A shorter T_1, or a longer T_2, than in vivo would give an erroneously good estimate of precision for the sequence. Proton density should also be comparable with that of tissue.

v) Each material should have high viscosity to reduce the effects of bulk movement. This can arise from convection (caused by temperature gradients), from the initial placing of the test object in the MR machine, or from vibration during imaging.

Water has been used widely as a standard; however, it has the following drawbacks: i) its diffusion coefficient at room temperature (2.0 10^{-9} m^2 s^{-1} at 20°C; 20) is considerably higher than the range of values found in normal brain (0.3–1.0 10^{-9} m^2 s^{-1} see above). Therefore, water measurements do not give a good indication of the precision of in vivo measurements. ii) water must be doped to bring its T_2 down to in vivo values; however, it must be established that the dopant has not significantly reduced the DC of the water. iii) the relatively low viscosity of water can cause problems (see above).

We identify a range of organic liquids as suitable materials for use as isotropic test objects for quantitative diffusion measurements. We report the diffusion coefficients, measured using a 4.7 T spectrometer, and other relevant characteristics for these liquids. These liquids could be used as diffusion standards world wide, for example in trials (21). The accuracy of a clinical diffusion imaging sequence (22) was also measured.

[1]NMR Research Unit, Department of Clinical Neurology, Institute of Neurology, Queen Square, University College London, London, UK.

[2]Centre for Medical and Health Physics, School of Physical Sciences, Queensland University of Technology, Brisbane, Australia.

Grant sponsors: Queensland University of Technology fellowship; Welcome Trust; Royal Society; Brain Research Trust; Multiple Sclerosis Society of Great Britain and Northern Ireland.

C.A. Clark's present address is Service Hospitalier Frederic Joliot, Departement de Recherche Medicale, CEA, 4 place du General-Leclerc, 91401 Orsay Cedex, France.

*Correspondence to: Paul Tofts, Institute of Neurology, Queen Square, London WC1N 3BG, UK. E-mail: p.tofts@ion.ucl.ac.uk

Received 30 April 1999; revised 23 September 1999; accepted 26 October 1999.

Table 1
Measurements of Diffusion Coefficient at 15–30°C Using a 4.7 T Spectrometer. Each Value Is the Average of 3 or 4 Measurements at the Same Temperature

	Diffusion coefficient ($10^{-9}m^2s^{-1}$)				McCall[a] 25°C	Viscosity[d] cp[e]
	15°C	20°C	25°C	30°C		
cyclohexane	1.214	1.345	1.474	1.652	1.4	0.89
cycloheptane	0.803	0.884	1.011	1.139	—	1.37
cyclooctane	0.432	0.498	0.564	0.653	—	1.96
n-octane	1.988	2.140	2.356	2.633	2.0	0.51
n-nonane	1.525	1.626	1.772	1.961	1.7	0.67
n-decane	1.165	1.268	1.386	1.559	1.3	0.84
n-undecane	0.931	1.009	1.112	1.248	—	1.10
n-dodecane	0.708	0.788	0.871	0.996	—	1.38
n-tridecane	0.565	0.640	0.707	0.805	—	1.72
n-tetradecane	0.443	0.495	0.550	0.637	—	2.13
n-pentadecane	0.357	0.404	0.461	0.535	—	2.54
n-hexadecane[b]	—	0.341	0.387	0.446	—	3.03
ethanol	0.850	0.977	1.080	1.218	1.0	1.07
n-propanol	0.455	0.536	0.627	0.720	0.6	1.95
n-butanol	0.336	0.397	0.456	0.542	0.5	2.54
water[c]	1.756	2.023	2.317	2.616	—	0.89

[a]Diffusion coefficient from McCall et al. (24), measured at 25°C, no uncertainties given.
[b]Solid at 15°C.
[c]At 30°C, only 2 measurements where taken; these agreed to within 0.1%.
[d]Viscosity at 25°C (28).
[e]NB 1 centipoise (cp) = 1 millipascal second.

METHODS

Choice of Liquids

The requirement for a single proton spectral line naturally guides us towards alkanes. Cyclic alkanes ($(CH_2)_n$ or C_nH_{2n} where n is the number of carbon atoms) consist of only methylene (CH_2) groups; thus, they have the advantage of a single spectral line. Cyclic alkanes are commercially available in a relatively small range (cycloheptane [$n = 5$] to cyclooctane [$n = 8$]). Three cyclic alkanes, from cyclohexane ($n = 6$) to cyclooctane ($n = 8$) were studied (see Table 1). The n-alkanes are linear, consisting of a chain of methylene groups, with a methyl (CH_3) terminus at each end (i.e., CH_3–$(CH_2)_{n-2}$–CH_3 or C_nH_{2n+2},). The n-alkanes are available in a large range of lengths, giving a good range of diffusion coefficients; the larger ones have a spectrum dominated by the methylene protons at 1.3 ppm (23); however, there is also a second resonance from the methyl protons (at 0.9 ppm), which may cause problems. Nine n-alkanes from n-octane ($n = 8$) to n-hexadecane ($n = 16$) were measured. Smaller alkanes are very volatile, and their diffusion coefficients are well above that of water; larger ones are solid at room temperature. Alcohols have been used previously (24); three n-alcohols (CH_3–$(CH_2)_{n-1}$–OH) were measured (ethanol [$n = 2$], 1-propanol [$n = 3$], and 1-butanol [$n = 4$]). These have more complex spectra; ethyl alcohol has three lines (CH_3, OH, and CH_2 lines at 1.2, 3.4, and 3.7 ppm, respectively), whereas 1-butanol has 5 lines (in the range 0.9–3.6 ppm). All these liquids are readily available from suppliers of laboratory chemicals. No weighing, mixing, or volume measurements are required. Standard procedures for handling these liquids include the use of basic protective equipment (gloves, eye protection, and white coat) in a well-ventilated room, or a fume cupboard in the case of larger quantities. Costs range from $13–40 (1999 prices) for 100 ml.

Measurements of Diffusion Coefficient Using a 4.7 T NMR Spectrometer

Measurements of the diffusion coefficient (DC) of the test liquids and also doped water ($T_1 \approx 113$ msec) were made on a Bruker MSL200 spectrometer at Queensland University of Technology, using a Bruker NMR microimaging probe and shielded gradient set inside the (15 cm diameter) horizontal bore of the 4.7 T superconducting magnet. The RF probe incorporated a 5-mm birdcage resonator. The liquid being measured was placed in a standard 5-mm NMR sample tube, to provide a sample length of approximately 5 mm. A vortex plug was also inserted to aid with field shimming and restrict the sample to the end of the tube.

A standard Stejskal-Tanner pulsed gradient spin echo sequence (25) was used, containing two gradient pulses (duration δ), with their start times separated by Δ, followed by a spin echo. Values of diffusion coefficient were measured at short echo time ($\delta = 4$ msec, $\Delta = 14$ msec, echo time TE = 28 msec) and long echo time ($\delta = 2.2$ msec, $\Delta = 47$ msec, TE = 94 msec). The repetition time was 2 sec. Six linearly incremented values of the gradient amplitude were used, to provide a graded attenuation of the signal, with attenuation down to approximately 1% at the highest gradient. To achieve this, the gradient increment value (and hence the range of b-values) was adjusted according to the value of the diffusion coefficient value being measured. Thus the smallest b-values were approximately 0.02/D, and the largest ones about 5/D. The attenuated signal S (in-phase component) was fitted to the expression:

$$S = S_o \exp(- \gamma^2 G^2 D \delta^2 (\Delta - \delta/3)) \quad [1]$$

where S_o is the unattenuated signal, G is the gradient amplitude, D is the diffusion coefficient, and S_o and D are the free parameters.

Shielded gradient coils with an internal diameter of 4 cm were used to provide switched gradients up to 700 mT m^{-1} (70 G/cm). Because the dimensions of these coils were much larger than the sample, the gradient was uniform within the sample. The *x*- and *z*-gradients were calibrated using a standard technique based on a sample of known dimensions. To assess any errors caused by variations in the gradients, either over time or between the different coils, the diffusion coefficient was always measured using two different gradient directions (*x*- and *z*-), and using two different echo times (short: TE = 28 msec and long: TE = 94 msec). In addition, the sum of residuals in the fit was monitored; if this was greater than approximately 0.5% in each point, the measurement was repeated.

Temperature control was achieved using a standard Bruker temperature controller. The system was calibrated using a thermocouple placed in the sample tube. We estimate the maximum uncertainty in temperature to be 0.3°C. Diffusion was measured at temperatures of 15, 20, 25, and 30°C.

4.7 T Diffusion Data Analysis

The temperature dependence of diffusion coefficients are often modelled by fitting to an Arrhenius activation law (20):

$$D = D_\infty \exp(- E_A/kT) = A \exp(- B/T) \quad [2]$$

where D_∞ is the diffusion coefficient in the limit of infinite temperature, E_A is the activation energy for translational diffusion of the molecules, k is Boltzmann's constant ($1.38\ 10^{-23}$ J K^{-1}), and T is the absolute temperature (K). $A = D_\infty$ and $B = E_A/k$ are treated as unknown parameters. The expression can be rearranged so that the diffusion coefficient D_o at a standard temperature T_o, near to the middle of the range of temperatures at which measurements were made, is one of the unknown parameters:

$$D = D_o \exp\left(- B\left(\frac{1}{T} - \frac{1}{T_o}\right)\right) ;\ D_o = D(T_o) \quad [3]$$

By taking natural logarithms, this becomes a linear problem. A quadratic term C can be added to model small deviations from Arrhenius behaviour:

$$\ln D = \ln(D_o) - B\left(\frac{1}{T} - \frac{1}{T_o}\right) + C\left(\frac{1}{T} - \frac{1}{T_o}\right)^2 \quad [4]$$

If C is zero, then simple linear squares regression of lnD vs. $(1/T - 1/T_o)$ gives *y*-intercept $\ln(D_o)$ and slope -B. Fitting ln(D) to a quadratic in $(1/T - 1/T_o)$ also gives the correction factor C . These procedures can be carried out exactly, without resorting to iteration.

Three models were examined for fitting the diffusion data. First, an Arrhenius (2-parameter) model over the whole temperature range (15–30°C) (i.e., Eq. [4] with C = 0); second, an Arrhenius model over the restricted temperature range 20–25°C; and third, a quadratic model over the whole temperature range (i.e., determining D_o, B, and C in Eq. [4]).

Fitting the values of ln(D) in this way, rather than the primary D values, is valid if there is equal absolute uncertainty in all ln(D) values, i.e., that all D values for a given liquid have the same *fractional* uncertainty. In the absence of any other information, this assumption is reasonable and leads to a considerable simplification of the data analysis. For a given liquid, D varies by only a factor of approximately 40% over the temperature range measured; thus, even if all D values had the same *absolute* uncertainty, the effect of the assumption would be small. T_o was set to 22°C, and values of D in the range 20–25°C were estimated.

The temperature coefficient (TC) of the diffusion coefficient was calculated from the value of B. Using Eq. [2], and ignoring nonideal behaviour (equivalent to ignoring the C term in Eq. [4]), the fractional increase in D per °C is:

$$TC = \left(\frac{1}{D}\right)\frac{\partial D}{\partial T} = \frac{B}{T^2} \quad [5]$$

To estimate the overall confidence limits in our estimated values of D, we considered three independent sources of error: random residuals in the fit, a systematic error in setting the temperature, and a systematic error in the gradient calibration.

The uncertainty in the *y*-intercept in Eq. [4], i.e., in $\ln(D_o)$, σ_A is given, for the 2-parameter model, by (26)

$$\sigma_A^2 = \sigma_y^2 \sum x_i^2 / (N \sum x_i^2 - (\sum x_i)^2) \quad [6]$$

where $\sigma_y{}^2$ = (residual sum of squares)/(N − 2), N is the number of points, and x_i are the measured *x*-values in the regression (assumed perfectly accurate). The expression for the 3-parameter model is similar, though more complex, and was evaluated with the help of Ref. 26. The fractional standard deviation in D_o, arising from scatter in the fit, is then equal to σ_A (since $\sigma_A = \sigma_{\ln Do} = \sigma_{Do}$ $(\partial \ln D_o/\partial D_o) = \sigma_{Do}/D_o$). The 95% confidence limit (95%CL) of fractional uncertainty in the estimate of diffusion coefficient at T_o, arising from scatter in the fit, is then $U_{fit} = 1.95\sigma_A$.

The fractional uncertainty in diffusion coefficient arising from a systematic error in setting the temperature is equal to the uncertainty in temperature (U_T°C, 95%CL) multiplied by the temperature coefficient TC. We estimate $U_T = 0.3$°C .

For the gradient calibration, two sources of error are relevant. The estimated 95% confidence limit on determining the slope of the calibration curve is 0.4%. For the sample dimensions it is 0.14% in the transverse (*x*- and *y*-) directions (since the diameter of the sample tube is specified by the manufacturer to a very high precision) and 0.7% in the longitudinal (*z*-) direction. Combining these, the maximum systematic uncertainty (95%CL) in the gradient amplitude, in measurements averaged from those using both the *x*- and *z*- gradients, is $U_G = 0.64\%$. The

fractional uncertainty in DC arising from the gradient calibration is then $2U_G$ (since G is squared in Eq. [1], e.g., a 1% error in G would give a 2% error in G^2).

The total uncertainty (95%CL) in the estimate of the diffusion coefficient U_{tot} is then given by combining the squares of the uncertainties from each of the three sources (assuming each uncertainty is uncorrelated):

$$U_{tot}^2 = U_{fit}^2 + TC^2U_T^2 + 4U_G^2 \qquad [7]$$

Systematic differences between D values measured using the *x*- and *z*-gradients were looked for. The maximum systematic difference in diffusion estimates (95%CL) can be estimated from the uncertainty in the gradient calibration factor (U_G) as follows. U_G is multiplied by 1.4 (because two measurements are being subtracted (27)), and by 2 (from the G^2 term in Eq. [1]). Thus, the difference could be as high as $2.8U_G$, i.e., 1.8% (using U_G = 0.64%; see above). Systematic differences between measurements from short and long echo times were also searched for.

Other Properties of the Liquids

Values for melting point, boiling point, viscosity, bulk density, and molecular weight (MWt) were collected from the literature (28,29). The proton density of each liquid was calculated, relative to that of water, from the density and the molecular formula. To assess consistency of the data from different liquids with each other, the dependence of D on molecular weight was investigated empirically.

Measurements of T_1 and T_2 at 1.5 T on a Clinical MRI System

The 15 liquids, in glass containers with polythene lids, were scanned in a loading annulus inside the head coil, with a tuning ring (supplied by the manufacturers). A slice-selective inversion recovery sequence (TR = 10 sec; TI = 0.1, 0.5, 1, 1.5, 2, 3, and 4 sec; TE = 14 msec) was used to measure T_1, with a 3-parameter fit. A 32-echo CPMG sequence (selective 90, hard 180° pulses, interecho interval 20 msec) was used to measure T_2, using a 3-parameter fit (to include odd-even echo differences). The accuracy of both methods was estimated to be ±5%.

Measurements of Apparent Diffusion Coefficient Using a 1.5 T MRI Sequence

The accuracy of an existing navigated pulsed gradient spin echo MRI sequence (22) was estimated using the liquids as test objects (i.e., assuming that the measurements made on the 4.7 T spectrometer are accurate). The sequence had δ = 25 msec, Δ = 31 msec, TE = 67 msec (for ADC measurement), TE = 81 msec (for navigation), G = 22 mTm^{-1}, b = 491 10^{-6} s m^{-2}, TR = 1 sec. The b-value calculation included contributions from the imaging gradients. The temperature of the liquids in the magnet bore (with no temperature control other than the room air conditioning) was estimated to be 23 ± 2°C . On a different occasion, measurements of water in a carefully controlled thermal environment had given D = 2.18 ± .01 10^{-9} m^2 s^{-1}(mean ± 95%CL) at 23 ± 1°C . This is very close to the data from Mills (20); interpolating the 15°C and 25°C values (1.777 and 2.299 $10^{-9}m^2s^{-1}$, respectively), assuming Arrhenius behaviour (Eq. [2]) gave D = 2.19 $10^{-9}m^2s^{-1}$ at 23°C.

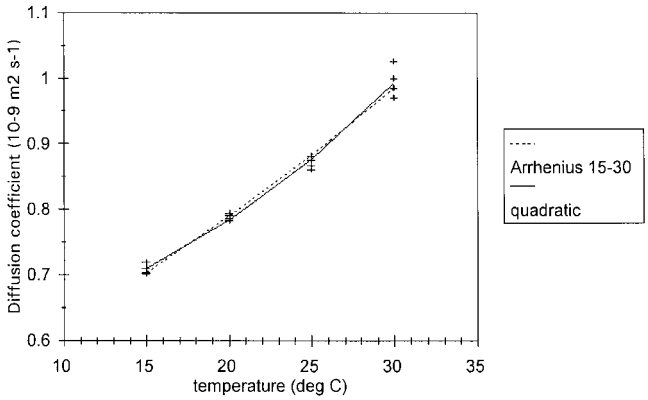

FIG. 1. Temperature dependence of diffusion coefficient of n-dodecane, showing the Arrhenius 15–30 model (Eq. [2]) and the quadratic model (Eq. [4]). The Arrhenius 20–25 model has been omitted for clarity; it usually lies very close to the quadratic model.

RESULTS

The basic 4.7 T diffusion data at each temperature, using the average of the 4 independent measurements (two echo times, two gradient directions), are shown in Table 1. Occasionally only 3 measurements were obtained. Published values of diffusion coefficient from McCall et al. (24) are also shown; no uncertainties were given; our values are in broad agreement with these. Our value for cyclohexane at 25°C agrees with that of Stilbs and Moseley (1.51 ± 0.03 10^{-9} m^2 s^{-1}) (30).

A typical plot for D vs. temperature T is shown in Fig. 1. The Arrhenius 15–30 model was usually slightly above the data at 20 and 25°C, and below it at 15 and 30°C; the Arrhenius 20–25 model was usually lower (by about 1%, ranging from 0–2%); the quadratic model usually coincided with the Arrhenius 20–25 model, and was lower than the Arrhenius 15–30 model. The fits for the quadratic model always looked convincing, and this model was chosen to interpolate the data. The fitted diffusion coefficients at temperatures between 20 and 25°C are shown in Table 2. Estimates of uncertainty arising from temperature had a mean of 0.7% (range 0.5–1.0%); those from gradient calibration were 1.3%; and those from fitting had a mean of 1.2% (range 0.4–2.2%). Total uncertainty in estimates of diffusion coefficient were in the range 1.4–2.7%. For alkanes it never exceeded 2.2%. Temperature coefficients were in the range 1.7–3.2%/°C (mean 2.3%/°C). (Le Bihan (31) found 2.8%/°C in a polyacrylamide gel). Values of diffusion coefficient at other temperatures near room temperature can be calculated by substituting the values of B and C into Eq. [4].

Systematic differences between measurements using the *x*-gradient coil and the *z*-gradient coil were small but significant. Combining signed fractional differences $(2(D_z - D_x)/(D_x + D_z))$ at short echo time (n = 45 values) and at long echo time (n = 57) gave a mean of 1.14% and stan-

Table 2
Diffusion Coefficients, PD, and T_1 and T_2 at 1.5 T for Test Liquids

Liquid	Formula	Diffusion coefficient ($10^{-9}m^2s^{-1}$)[a]						U_T %[b]	TC[c] %/°C	T_1	T_2[e]	B[f] K	C[f] 10^6K^2	PD[h]
		20°C	21°C	22°C	23°C	24°C	25°C			ms at 1.5 T[d]				
cyclohexane	C_6H_{12}	1.338	1.365	1.393	1.422	1.451	1.482	1.9	2.0	2328	1329	1764	1.35	1.00
cycloheptane	C_7H_{14}	0.891	0.912	0.933	0.955	0.979	1.003	2.1	2.4	2156	1598	2048	2.38	1.05
cyclooctane	C_8H_{16}	0.495	0.509	0.523	0.538	0.552	0.568	1.9	2.7	1608	1234	2382	0.88	1.08
n-octane	CH_3-$(CH_2)_6$-CH_3	2.141	2.179	2.219	2.261	2.306	2.354	1.5	1.9	1932	193	1615	3.35	1.00
n-nonane	CH_3-$(CH_2)_7$-CH_3	1.627	1.652	1.679	1.708	1.738	1.770	1.4	1.7	1748	140	1442	3.27	1.01
n-decane	CH_3-$(CH_2)_8$-CH_3	1.263	1.286	1.310	1.336	1.363	1.391	1.6	1.9	1526	145	1658	2.98	1.02
n-undecane	CH_3-$(CH_2)_9$-CH_3	1.009	1.027	1.047	1.068	1.090	1.113	1.8	1.9	1331	204	1681	3.13	1.03
n-dodecane	CH_3-$(CH_2)_{10}$-CH_3	0.783	0.800	0.818	0.837	0.856	0.876	1.8	2.2	1160	163	1937	2.55	1.03
n-tridecane	CH_3-$(CH_2)_{11}$-CH_3	0.634	0.649	0.664	0.680	0.696	0.712	2.2	2.3	999	173	2019	1.05	1.04
n-tetradecane	CH_3-$(CH_2)_{12}$-CH_3	0.491	0.502	0.514	0.526	0.540	0.554	1.8	2.4	869	198	2056	3.44	1.04
n-pentadecane	CH_3-$(CH_2)_{13}$-CH_3	0.403	0.414	0.425	0.437	0.449	0.462	1.9	2.7	751	178	2323	2.69	1.05
n-hexadecane	CH_3-$(CH_2)_{14}$-CH_3	0.341	0.349	0.358	0.367	0.377	0.387	1.9	2.5	669	201	2173	3.26	1.05
ethanol	C_2H_5OH	0.969	0.993	1.017	1.041	1.065	1.090	2.0	2.4	2141	20[i]	2061	−0.91	0.93
1-propanol	C_3H_7OH	0.537	0.554	0.572	0.590	0.608	0.626	2.2	3.1	1405	31[j]	2692	−1.19	0.97
1-butanol	C_4H_9OH	0.393	0.406	0.419	0.432	0.446	0.461	2.7	3.2	1149	68	2742	1.13	0.99
water[g]	H_2O	2.026	2.082	2.139	2.197	2.255	2.314	1.5	2.7	2600	1370	2328	−0.82	1.00

[a]Interpolated from 4.7T spectrometer data in Table 1 (see text).
[b]Total uncertainty (95%CL) in diffusion coefficient.
[c]Temperature coefficient.
[d]22°C.
[e]Mono-expontial T_2 fit (transverse magnetisation decay curve may have j-modulation-see text).
[f]See Eq. [4]; T_0 = 22°C (295K).
[g]Distilled water, not deoxygenated.
[h]Proton Density, calculated from density and molecular formula; relative to water.
[i]Fitted to 4 echoes up to TE = 80ms.
[j]Fitted to 5 echoes up to TE = 100ms.

dard error of 0.23%. This measured systematic difference is significant, but well within the expected limits (1.8% see above), given the uncertainty in the individual gradient calibration factors. Systematic differences between short and long echo times (over all four temperatures) were not significant; the mean fractional difference $2(D_{long} - D_{short})/(D_{long} + D_{short}) = 0.16\%$, standard error = 0.2%.

Water DC values showed very little scatter at a given temperature. The uncertainty (95%CL) arising from the lnD vs. T fit was 0.23%, half that of any other liquid. Mills (20) measured the self diffusion coefficient of water using a (non-NMR) diaphragm cell technique, considered to be accurate to ±0.2%. Temperature was controlled to within 0.01°C. He found $D = 1.777\ 10^{-9}m^2s^{-1}$ at 15°C and $D = 2.299\ 10^{-9}m^2s^{-1}$ at 25°C. Thus, our values (Table 1) differ by −1.2% (15°C) and +0.8% (25°C), respectively; and agree within the estimated uncertainty (1.5% see Table 2).

The melting points were all below 12°C, with the exception of n-hexadecane, which melts at 18°C. Boiling points were all above 77°C. Viscosities are shown in Table 1. Bulk densities for the organic liquids ranged from 0.70−0.83 g ml^{-1}. European Community safety categories for the range of liquids were: flammable, highly flammable, harmful by inhalation, and irritating to eyes, respiratory system, and skin . A log-log plot of D vs. molecular weight (Fig. 2) shows a very smooth behaviour for the n-alkanes, suggesting that random errors in the measurements are small. Linear regression of $\log_{10}D$ vs. $\log_{10}MWt$ indicated a $MWt^{-2.66}$ dependence for D. The curves for cyclic alkanes and alcohols are less regular; this is presumably caused by their small size, and is consistent with the irregular behaviour of their melting and boiling points.

T_1 and T_2 values at 1.5 T are shown in Table 2. Water values were T_1 = 2.60 sec, T_2 = 1.37 sec, consistent with published values for water (32) (given that it had not been deoxygenated). The CPMG plots up to 640 msec for all the liquids except ethanol and 1-propanol fitted a monoexponential decay with a maximum residual of 2% of the initial value. The echo trains from two smaller alcohols (ethanol and 1-propanol) showed complex J-modulation behaviours; an effective T_2 value was estimated from the first 80−100 msec of data.

Diffusion coefficient measurements made with the MRI sequence at 1.5 T agreed well with the 4.7 T spectroscopic data, indicating that it is accurate to within the experimental error (Fig. 3). The mean (signed) difference was −2.1%.

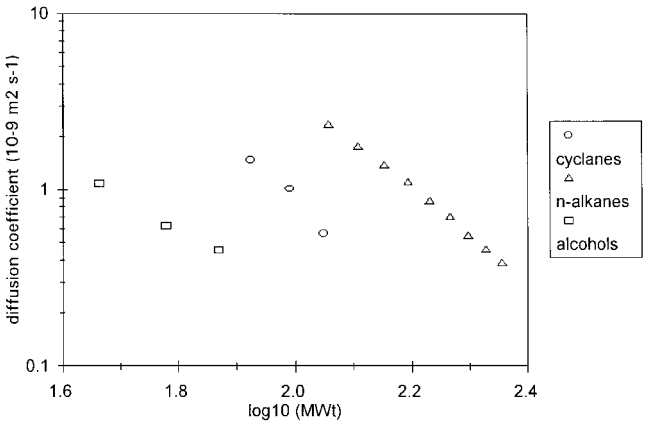

FIG. 2. Measured diffusion coefficient (at 25°C) vs. molecular weight (log-log plot).

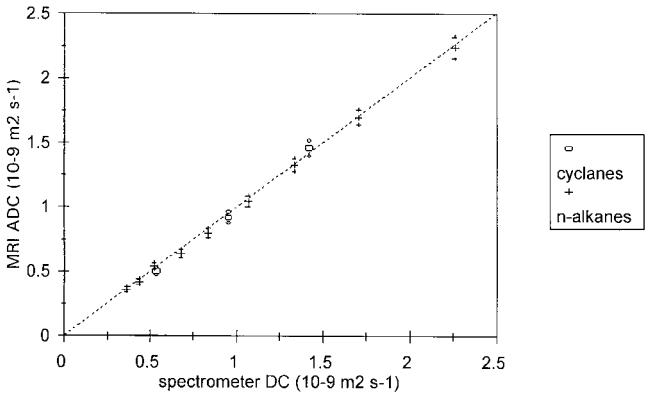

FIG. 3. The accuracy of MRI ADC values, estimated by comparison with values measured using a 4.7 T spectrometer. The mean signed difference is −2.1%. The large symbols are the MRI values measured at an estimated 23°C; the small symbols show the uncertainty in these MRI values arising from an uncertainty of 2°C in the measurement temperature, using the temperature coefficients in Table 2. The spectroscopic values are estimated to have maximum uncertainty of ±2%.

DISCUSSION

The long cyclic alkanes have useful diffusion coefficients, although their T_1 and T_2 values are unrealistically long. The n-alkanes cover the required range of diffusion coefficient, with reasonable values of T_1 and T_2. The alcohols also have useful diffusion coefficients. All the liquids have proton density values near to that of water. All except four of the test liquids have higher viscosity than water (Table 3); the exceptions are the light alkanes cyclohexane, n-octane, n-nonane, and n-decane, which have high DCs (1.4 10^{-9} m s^{-1} or more), above that of normal white matter, and approach that of water (Tables 1 or 2). The alcohols have short effective T_2 values (Table 2) and complex spectra (CH_2, CH_3, and OH lines) which probably rule them out as useful test liquids.

The current 4.7 T spectrometer methodology has provided an uncertainty of approximately 2%. With more stable gradient current amplifiers, magnitude signal detection, and a specially constructed probe to provide well-defined sample dimensions, and a more isothermal environment for the sample, the total uncertainty in DC could probably be reduced to less than 1%.

All the liquids are safe to handle, provided appropriate straightforward precautions are taken. They are well-defined, stable, and readily available. The liquids can be stored and measured in readily available standard containers. A small amount of evaporation is not a problem, because the liquids are not mixtures (as gels are), and therefore evaporation will not alter the composition of the remaining liquid.

Aqueous solutions of sucrose, agar (33) or glycerol have been proposed. We have avoided these because of the amount of on-site laboratory work required in making up the solutions, the difficulty in ensuring that the manufacturing process is consistent across sites and over time, the possibility of the mixtures losing water over time, and the possibility of microbial or fungal attack. In our own commercially manufactured gel standards (34), T_1 and T_2 have changed by approximately 10% over approximately 5 years. Spatially uniform gels may be hard to manufacture. In addition, the minimum DC that can be obtained may be too high to simulate that seen in ischaemic brain (e.g., agar goes down to 1.7 10^{-9} m^2 s^{-1}, and sucrose down to 1.0 10^{-9} m^2 s^{-1} (33), both well above that of normal white matter and acutely ischemic tissue).

We recommend that clinical sequences for the measurement of ADC or diffusion tensor should be tested with this range of alkanes (cyclic and linear), to characterize both precision and accuracy, in ongoing quality assurance programs. In particular, n-tridecane has a diffusion coefficient close to that of normal white matter.

ACKNOWLEDGMENTS

P.S.T. received support from a Queensland University of Technology visiting fellowship, the Welcome Trust and the Royal Society. CAC was supported by the Brain Research Trust. G.J.M.P., G.J.B. and the 1.5 T MR scanner at UCL are supported by the Multiple Sclerosis Society of Great Britain and Northern Ireland. Helpful discussions took place with members of the European MAGNIMS group studying MR and MS (European Community grant ERBCHRXCT94-0684) and with Carlo Pierpaoli.

REFERENCES

1. Taylor DG, Bushell MC, The spatial mapping of translational diffusion coefficients by the NMR imaging technique. Phys Med Biol 1985;30: 345–349.
2. Merboldt KD, Hanicke W, Frahm J. Self-diffusion NMR imaging using stimulated echoes. J Magn Reson 1985;64:479–486.
3. Le Bihan D, Breton E. Imagerie de diffusion in vivo par resonance magnetique nucleaire. C R Acad Sci Paris 1985;301:1109–1112.
4. Le Bihan D, Breton E, Lallemand D, Aubin M, Vignaud J, Laval-Jeantet M. Separation of diffusion and perfusion in intravoxel incoherent motion MR imaging. Radiology 1988;168:497–505.
5. Moseley ME, Cohen Y, Mintorovitch J, Chileuitt L, Shimizu H, Kucharczyk J, Wendland MF, Weinstein PR. Early detection of cerebral ischemia in cats: comparison of diffusion- and T_2-weighted MRI and spectroscopy. Magn Reson Med 1990;14:330–346.
6. Warach W, Chien D, Li W, Ronthal M, Edelman RR. Fast magnetic resonance diffusion-weighted imaging of acute human stroke. Neurology 1992;42:1717–1723.
7. Werring DJ, Clark CA, Barker GJ, Thompson AJ, Miller DH. Diffusion tensor imaging of lesions and normal appearing white matter in multiple sclerosis. Neurology 1999;52:1626–1632.
8. Wieshmann UC, Clark CA, Symms MR, Barker GJ, Birnie KD, Shorvon SD. Water diffusion in the human hippocampus in epilepsy. Magn Reson Imaging 1999;17:29–36.
9. Tsuruda JS, Chew WM, Moseley ME, Norman D. Diffusion-weighted MR imaging of the brain: value of differentiating between extraaxial cysts and epidermoid tumours. Am J Neuroradiol 1990;11:925–931.
10. Neil JJ, Shiran SI, McKinstry RC, Schefft GL, Snyder AZ, Almli CR, Akbudak E, Aronovitz JA, Miller JP, Lee BCP, Conturo TE. Normal brain in human newborns: apparent diffusion coefficient and diffusion anisotropy measured by using diffusion tensor MR imaging. Radiology 1998;209:57–66.
11. Poupon C, Clark CA, Frouin V, Bloch I, Le Bihan D, Mangin J. Tracking white matter fascicles with diffusion tensor imaging. In: Proceedings of the 7th Annual Meeting of the ISMRM, Philadelphia, 1999. p 325.
12. Chien D, Buxton RB, Kwong KK, Brady TJ, Rosen BR. MR diffusion imaging of the human brain. J Comp Assist Tomogr 1990;14:514–520.
13. Basser PJ, Le Bihan D, Mattiello J. Estimation of the effective self-diffusion tensor from the NMR spin echo. J Magn Reson Series B 1994;103:247–254.
14. Basser PJ, Pierpaoli C. Microstructural and physiological features of tissues elucidated by quantitative-diffusion-tensor MRI. J Magn Reson Series B 1996;111:209–219.

15. Pierpaoli C, Basser PJ. Toward a quantitative assessment of diffusion anisotropy. Magn Reson Med 1996;36:893–906.
16. Marks MP, de Crespigny A, Lentz D, Enzmann DR, Albers GW, Moseley ME. Acute and chronic stroke: navigated spin-echo diffusion-weighted MR imaging. Radiology 1996;199:403–408.
17. Pierpaoli CP, Jezzard P, Basser PJ, Barnett A, Di Chiro G. Diffusion tensor MR imaging of the human brain. Radiology 1996;201:637–648.
18. Droogan AG, Clark CA, Werring DJ, Barker GJ, Miller DH. Navigated spin echo diffusion-weighted imaging in clinical phenotypes of multiple sclerosis. In: Proceedings of the 6th Annual Meeting of ISMRM, Sydney, Australia, 1998. p 117.
19. de Certaines JD, Henriksen O, Spisni A, Cortsen M, Ring PB . In vivo measurements of proton relaxation times in human brain, liver and skeletal muscle: a multicenter study. Magn Reson Imaging 1993;11: 841–850.
20. Mills R. Self-diffusion in normal and heavy water in the range 1–45°. J Phys Chem.1973;77:685–688.
21. Tofts PS. Standardization and optimization of MR techniques for multicenter studies. J. Neurology Neurosurgery and Psychiatry 1998; 64(suppl 1):S37–43.
22. Clark CA, Droogan A, Anderson AW, Barker GJ, Tofts PS. Diffusion imaging of multiple sclerosis plaques using a navigated PGSE. In: Proceedings of the 5th Annual Meeting of the ISMRM, Vancouver, Canada, 1997. p 1715.
23. Pouchert CJ, Behnke J. The Aldrich library of ^{13}C and ^{1}H FT-NMR spectra. Milwaukee, WI: Aldrich Chemical; 1992.
24. McCall DW, Douglass DC, Anderson EW. Diffusion in liquids. J Chem Physics 1959;31:1555–1557.
25. Stejskal EO, Tanner JE. Spin diffusion measurements: spin echoes in the presence of a time-dependent field gradient. J Chem Phys 1965;42: 288–292.
26. Taylor JR. An introduction to error analysis, 2nd edition. Sausalito, CA: University Science Books; 1997. p 188.
27. Bland JM, Altman DG. Measurement error. Br Med J 1996;312:1654
28. Lide DR, editor-in-chief. CRC handbook of chemistry and physics, 78th edition. New York: CRC Press; 1997.
29. Windolz M, editor. The Merck Index, 10th edition. Rahway, NJ: Merck & Co.; 1983.
30. Stilbs P, Moseley ME. Nuclear spin-echo experiments on standard Fourier transform NMR spectrometers. Chemica Scripta 1978;13:26–28.
31. Le Bihan D, Delannoy J, Levin RL. Temperature mapping with MR imaging of molecular diffusion: application to hyperthermia. Radiology 1989;171:853–857.
32. Cowan B. Nuclear magnetic resonance and relaxation. Cambridge, UK: Cambridge University Press; 1997. p 237.
33. Laubach HJ, Jakob PM, Loevblad KO, Baird AE, Bovo MP, Edelman RR, Warach S. A phantom for diffusion-weighted imaging of acute stroke. J Magn Reson Imaging 1998;8:1349–1354.
34. Walker P, Lerski RA, Mathur-De Vre R, Binet J, Yane F. Identification and characterisation of biological tissues by NMR: VI. Preparation of agarose gels as reference substances for NMR relaxation time measurement. Magn Reson Imaging 1988;6:215–222.